Presence of telomeric G-strand tails in the telomerase catalytic subunit *TERT* knockout mice

Xunmei Yuan[1], Shun Ishibashi[2], Shinji Hatakeyama[1], Motoki Saito[1], Jun-ichi Nakayama[1], Rika Nikaido[1], Takahiro Haruyama[3], Yoshifumi Watanabe[3], Hijiri Iwata[4], Mari Iida[4], Haruhiko Sugimura[5], Nobuhiro Yamada[2] and Fuyuki Ishikawa[1,*]

[1]*Graduate School of Bioscience and Biotechnology and* [3]*Department of Biomolecular Engineering, Tokyo Institute of Technology, 4259 Nagatsuta, Midori-ku, Yokohama, 226-8501, Japan*

[2]*Department of Metabolic Diseases, Faculty of Medicine, University of Tokyo, 7-3-1 Hongo, Bunkyo-ku, Tokyo 113-8655, Japan*

[4]*Biosafety Research Center, Foods, Drugs, and Pesticides, 583-2 Arahama, Shioshinden, Fukude-cho, Iwata, Shizuoka 437-1213, Japan*

[5]*The First Department of Pathology, Hamamatsu University School of Medicine, 3600 Handa-cho, Hamamatsu, 431-3192, Japan*

Abstract

***Background*: Telomerase consists of two essential subunits, the template RNA (TR; telomerase RNA) and the catalytic subunit TERT (telomerase reverse transcriptase). Knockout mice with a *mTR* (mouse *TR*) deletion have been described and well characterized. However, mice with a *mTERT* (mouse *TERT*) deletion have not been reported.**

***Results*: *mTERT*-knockout mice have been constructed. The first generation *mTERT*$^{-/-}$ mice were fertile, and did not show any noticeable macroscopic or microscopic phenotypic change. All tissue cells derived from *mTERT*$^{-/-}$ mice that were examined lacked telomerase activity, indicating that *mTERT* is the only gene encoding the telomerase catalytic subunit. Pulse field gel electrophoresis (PFGE) and nondenaturing in-gel hybridization analyses showed that mouse telomeric DNA has G-strand 5′-overhangs, as demonstrated for human and yeast cells. This telomeric single-stranded G-tail was also observed in MEF (mouse embryonic fibroblast) and liver cells derived from *mTERT*$^{-/-}$ mice.**

***Conclusions*: *mTERT*-knockout mice show phenotypes that are apparently normal at least during the early generations. This observation is similar to that obtained with the *mTR*-knockout mice. The presence of the telomeric G-strand tails in *mTERT*$^{-/-}$ mice suggests that these telomeric 5′-overhangs are produced by telomerase-independent mechanisms, as has been proposed for yeast and human.**

Introduction

Telomerase is a reverse transcriptase that catalyses the *de novo* synthesis of telomeric repeats (Greider & Blackburn 1985; Nugent *et al.* 1998). It compensates for the inability of conventional DNA polymerases to replicate the extreme ends of telomeres (end replication problem). Telomerase activity is strictly regulated in normal cells: It is active in germ cells, embryonic tissues, activated lymphocytes and stem cells, but inactive in most somatic cells. In contrast, telomerase is activated in about 90% of clinical cancers and cell lines (reviewed in Shay & Bacchetti 1997). Therefore, it has been postulated that telomerase is necessary for proliferating cells to maintain cell division by resolving the end replication problem. At the same time, the absence of telomerase in most normal human somatic cells has suggested that excessive telomerase activity may have some disadvantages, such as the induction of cancers in individuals.

Telomerase contains two components; the catalytic protein TERT (telomerase reverse transcriptase)

Communicated by: Kohei Miyazono

* *Correspondence:* E-mail: fishikaw@bio.titech.ac.jp

(Counter *et al.* 1997; Lingner *et al.* 1997; Meyerson *et al.* 1997) and the template RNA TR (telomerase RNA) (Greider & Blackburn 1989; Yu *et al.* 1990; Blasco *et al.* 1995; Feng *et al.* 1995). *In vitro* transcribed TR and the recombinant TERT protein produced in a reticulocyte lysate reconstitute the telomerase activity (Weinrich *et al.* 1997). Therefore, these two factors are essential and sufficient for telomerase activity, at least as measured *in vitro*. The telomerase-associated protein TEP1 has been reported (Harrington *et al.* 1997; Nakayama *et al.* 1997), but its function remains unknown.

One direct way of clarifying the functions of a particular enzyme is to look at the phenotype of knockout mice. Knockout mice for the *mTR* (mouse TR) gene have been reported (Blasco *et al.* 1997). $mTR^{-/-}$ mice were viable, fertile and apparently normal until the fifth generation. However, in later generations they showed aneuploidy, chromosomal end fusions, hypotrophic gonads due to extensive apoptosis, accelerated ageing, and they become infertile at the sixth generation (Lee *et al.* 1998). These adverse effects on cell growth have not been observed in $p53^{-/-}$ $mTR^{-/-}$ double knockout mice (Chin *et al.* 1999), suggesting that p53 acts downstream to signal the reduction in telomere length to the cell cycle and apoptosis machineries.

Knockout mice for another essential component for telomerase, the TERT catalytic subunit, have not been reported. TERT is a protein with a mass of about 110 kDa. The N-terminal half of the TERT proteins is rich in basic amino acids, although the function of this region remains unknown. Notably, the C-terminal half contains the 1 2, A, B′, C and D motifs, which are highly conserved among reverse transcriptases of diverse origins. The A and B′ motifs in particular include the aspartic acid residues that are believed to form the catalytic centre of the reverse transcriptase, and are essential for activity (Lingner *et al.* 1997; Nakayama *et al.* 1998).

To understand the biological role of TERT *in vivo*, we have constructed *TERT*-knockout mice. This paper describes the initial characterization of the knockout mice. Specifically, we have focused on the role of the TERT protein in forming the terminal G-strand tails of telomeric DNA.

Results

Generation of *mTERT* knockout mice

We have identified mouse *TERT* (*mTERT*) genomic clones from a phage library constructed using the 129Sv mouse DNA. The approximately 30-kb *mTERT* region was deduced from the composite of three independent genomic clones, and a 14-kb subclone was analysed in detail. Nucleotide sequencing and Southern blotting experiments using the *mTERT* cDNA as a probe indicated that this 14-kb region contains 10 exons (exons α–κ in Fig. 1A; Note that we do not know the relative positions of these exons within the total *mTERT* gene). We constructed a targeting vector in which the 4-kb *Bam*HI fragment containing exons γ, δ and ϵ was replaced by the neomycin resistance gene *neo* (Fig. 1A). Exon γ codes for part of motif A of the mTERT protein (amino acids 701–753 of mTERT) (Fig. 1B). In this motif, Asp^{702} is highly conserved among reverse transcriptases, including the TERT proteins of various species, and it comprises the catalytic centre of the enzyme (shown by an asterisk in Fig. 1B). A mutant *hTERT* cDNA substituting Ala at Asp^{702} was shown to be totally defective in telomerase activity (Nakayama *et al.* 1998). Therefore, knockout mice producing a mutant TERT protein devoid of this region were expected to be defective for telomerase activity.

The targeting vector was introduced into the JH1 ES cells strain, and 15 independent ES sublines that had undergone homologous recombination and were heterozygous for the targeted gene were isolated. These independent ES lines were injected into C57BL/6 blastocysts, and chimeric mice that transmitted the targeted allele through the germ-line were obtained from two independent lines. These two founder mice produced heterozygous progeny by mating with C57BL/6 wild-type mice. Thus made heterozygous mice were then intercrossed for each of founder lines to produce mice homozygous for the targeted allele. Figure 1C shows a representative Southern blotting analysis using the KH probe shown in Fig. 1A to analyse the genotypes of mice obtained from three independent intercrosses between heterozygous mice. As expected, the wild-type and targeted alleles produced 2.2 kb and 3.4 kb *Bam*HI fragments, respectively. The lack of extra-bands common to the three genotypes indicated that *mTERT* is a single copy gene. In all heterozygous mice matings, the wild-type, heterozygous and homozygously targeted mice were obtained at the frequencies expected from Menderian inheritance (1 : 2 : 1.1, respectively; a result calculated from 401 mice). Therefore, it was suggested that the targeted *mTERT* genotype did not have any effect on mouse embryonic development. The two *mTERT*-targeted mouse lines derived from the two ES lines showed essentially the same phenotypes, and in this report we will describe one line in detail.

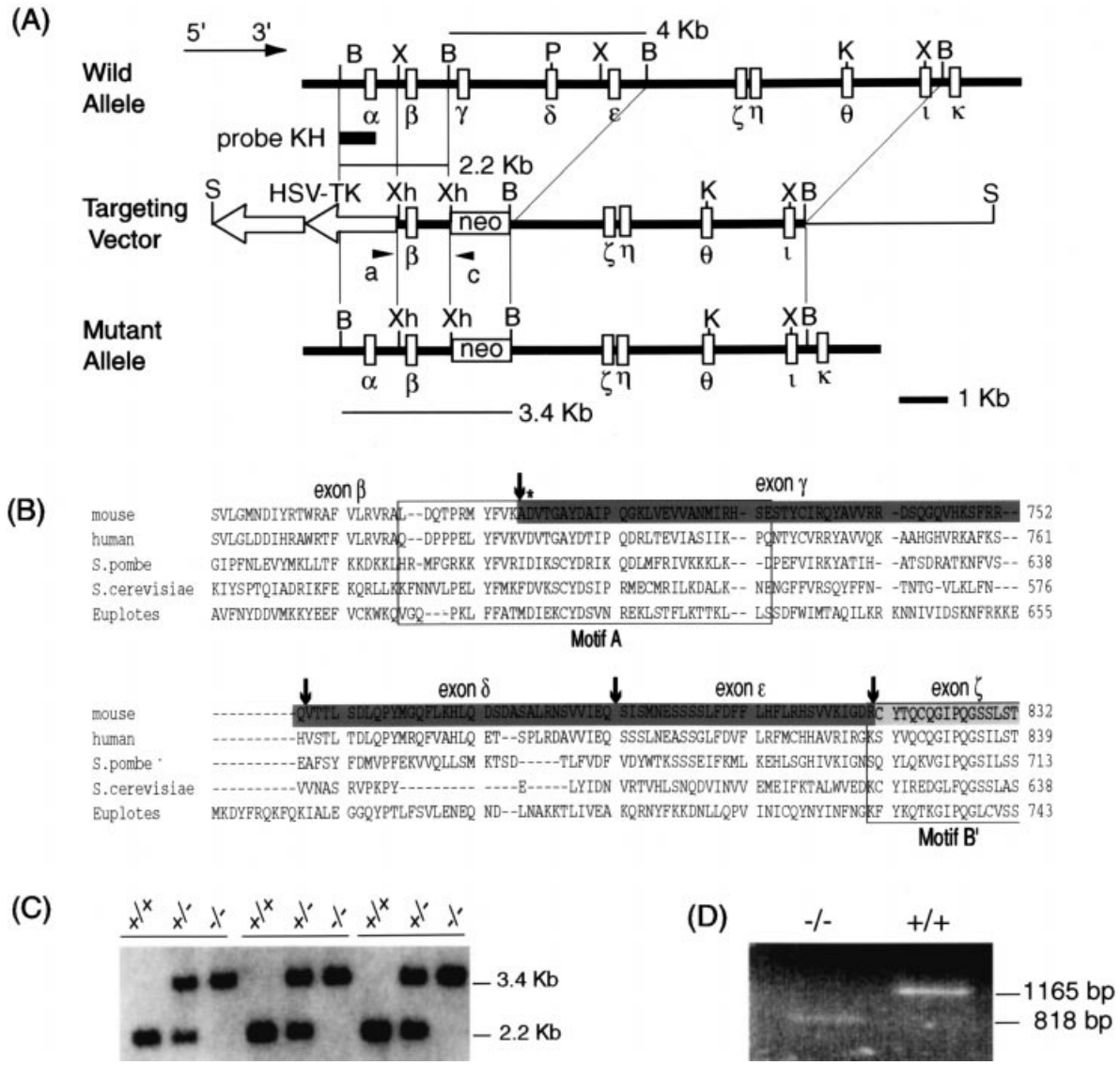

Figure 1 Disruption of the *mTERT* gene. (A) Targeting vector. A 14-kb *mTERT* genomic DNA containing exons α through κ is shown in the top panel, and the targeting vector and the expected targeted allele are shown in the middle and bottom panels, respectively. The targeting vector was constructed by replacing the 4-kb *Bam*HI fragment containing exons γ, δ and ε with the neomycin resistant gene (neo). This replacement produced a 3.4-kb *Bam*HI fragment detected by the probe KH in the targeted allele, whereas the wild-type allele gave rise to a 2.2-kb fragment. The position of the HSV-TK gene used as a negative selection marker for gene targeting, and those of the two PCR primers a and c used for genotyping (see experimental procedures) are also shown. Abbreviations for restriction enzymes are B, *Bam*H I; K, *Kpn*I; P, *Pst*I; S, *Sph*I; X, *Xba*I; Xh, *Xho*I. (B) Alignment of the mouse, human, *S. pombe, S. cerevisiae and Euplotes* TERT motif A and B′ amino acid sequences. The positions of introns (vertical arrows) and the corresponding exons are shown. Motif A and part of B′ are boxed. The deleted amino acids (heavy hatching) and the downstream missensed amino acids (light hatching) in the mutant protein are indicated. An asterisk denotes the Asp^{702} that is highly conserved among reverse transcriptases, and essential for telomerase activity. (C) Southern blot analysis of $mTERT^{+/+}$, $mTERT^{+/-}$, and $mTERT^{-/-}$ mice. Probe KH (shown in A) was used for Southern blot analysis of tail DNAs derived from three independent littermates. Arrows on the right indicate the 3.4-kb *Bam*HI fragment of the targeted allele and the 2.2-kb fragment of the wild-type allele. (D) RT − PCR analysis of the *TERT* transcripts derived from $mTERT^{+/+}$ and $mTERT^{-/-}$ mice. RT-PCR analysis was performed using primers located in the exon α and κ. Arrows on the right indicate the 1165-bp and 818-bp PCR products obtained from the targeted and wild-type alleles.

The *mTERT* transcripts derived from the wild-type and targeted alleles were examined by RT-PCR using two primers located in exon α and κ. Using these primers, 1165-bp and 818-bp fragments were obtained from the wild-type and homozygously targeted mice, respectively. Nucleotide sequencing of the products indicated that the targeted allele produced mRNA with a 347 nucleotide deletion, which corresponds to exons γ, δ and ϵ (nucleotide 2101–2447 of GENBANK accession number AF073311), as expected. This deletion results in a frame-shift of the open reading frame after Cys^{817}, which is immediately followed by a premature termination codon.

Telomerase activity in *mTERT* knockout mice

We next examined the telomerase activities in the testis, liver and MEF (mouse embryonic fibroblast) cells for the wild-type, heterozygous and homozygously targeted mice (Fig. 2). The quantitative stretch PCR assay (Tatematsu *et al.* 1996) detected significant levels of telomerase activity in the testis, liver and MEF cells derived from the wild-type mice. Intermediate levels of activity were detected in those cells derived from the heterozygous mice, and no activity was found in the homozygously targeted mice. Telomerase activity was not detected in brain and heart in any of the case (data not shown). Since the targeted allele does not produce functional telomerase, we hereafter refer to the homozygously targeted mice as $mTERT^{-/-}$.

No macroscopic or microscopic change in the first generation of *mTERT* knockout mice

The first generation of the $mTERT^{-/-}$ mice did not show any appreciable gross phenotypic changes when compared to their wild-type and heterozygous littermates. Testis (Fig. 3), ovary, brain, gastrointestinal tract, liver, pancreas, adrenals, hypophysis, submandibular glands, thyroid, parathyroid, thymus, spleen, bone marrow, kidneys, lungs and heart were examined microscopically and no significant pathological change was observed (data not shown). $mTERT^{-/-}$ mice were fertile, and intercrosses between two first-generation (G1) $mTERT^{-/-}$ mice produced the second generation (G2) of $mTERT^{-/-}$ mice. These littermate sizes were similar to those obtained by wild-type intercrosses, again suggesting that the absence of functional mTERT protein had no effect on embryo development, at least in G1 and G2. The normal phenotypes observed for $mTERT^{-/-}$ mice in earlier generations are reminiscent of those observed for the $mTR^{-/-}$ mice.

mTR expression levels in $mTERT^{-/-}$ mice

Recently, it has been reported that human normal fibroblast cells expressing an exogenous *hTERT* contained approximately twice as much hTR as did their corresponding telomerase-negative parental cells (Yi *et al.* 1999). However, this comparison was made

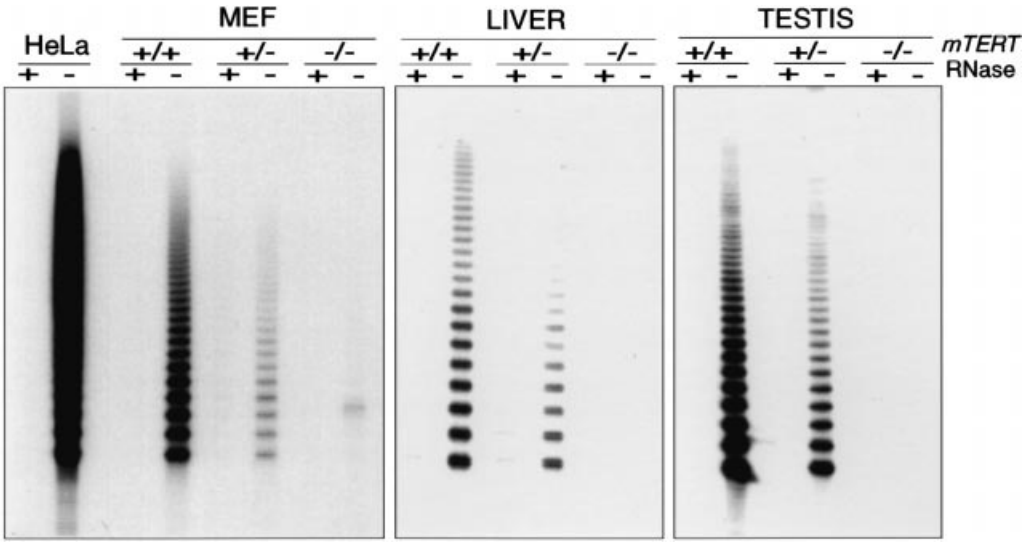

Figure 2 Telomerase activity in $mTERT^{+/+}$, $mTERT^{+/-}$, and $mTERT^{-/-}$ mice. Telomerase activities were analysed by the stretch PCR assay for MEF cells, testes and livers from the $mTERT^{+/+}$, $mTERT^{+/-}$ and $mTERT^{-/-}$ mice. HeLa cell extract was used as a positive control, and the specificity of the telomerase reactions was confirmed by RNase treatment of extracts prior to the reactions.

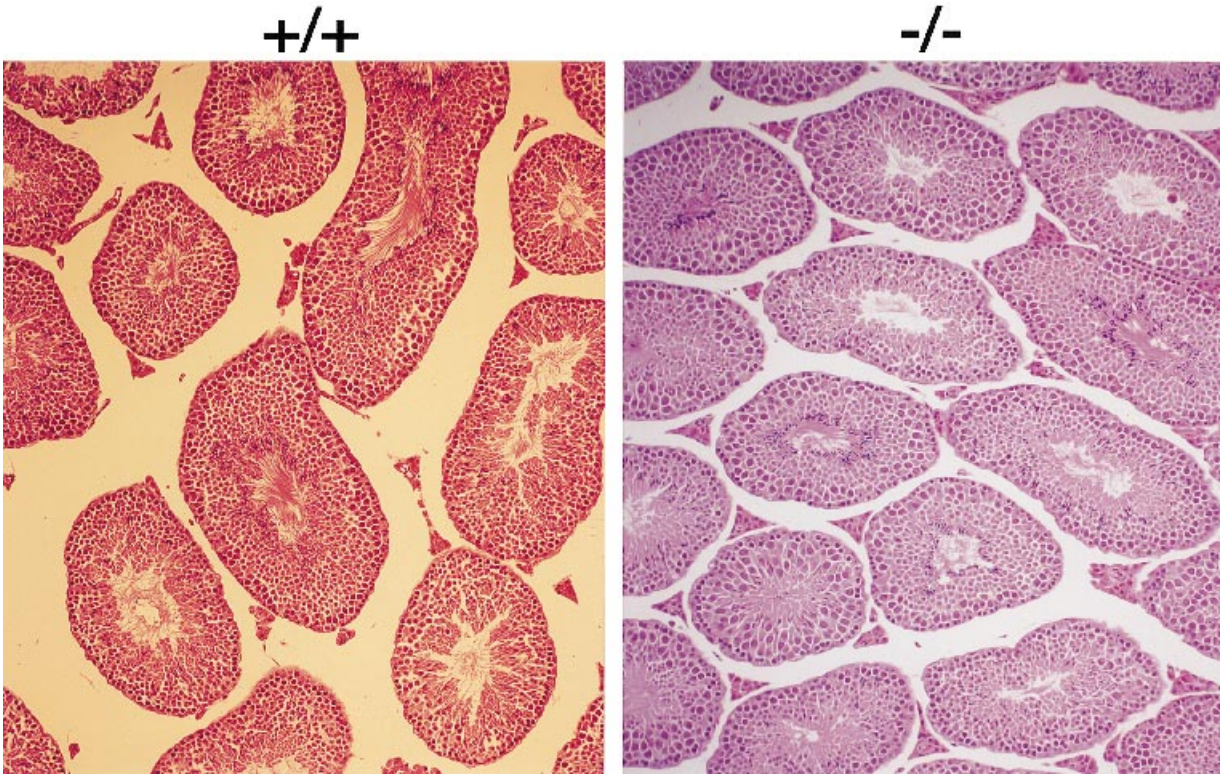

Figure 3 Histological analyses of testes from adult $mTERT^{+/+}$and $mTERT^{-/-}$ littermates. Hematoxylin-Eosin stained section of $mTERT^{-/-}$ testis (right panel) shows normal cellularity and tubules undergoing active spermatogenesis compared to that of the wild-type testis (left panel).

between two normal human fibroblast sublines maintained differently *in vitro*, and the observed different *mTR* expression levels may have been related to the difference of growth conditions, such as growth rates, of these two types of cells. Normal mouse embryos actively express the *mTERT* gene. Nevertheless, as stated earlier, the G1 $mTERT^{-/-}$ embryos developed normally as their $mTERT^{+/+}$ and $mTERT^{+/-}$ siblings. Moreover, we did not find any difference in growth kinetics among $mTERT^{+/+}$, $mTERT^{+/-}$ and $mTERT^{-/-}$ MEF cells *in vitro* (data not shown). Therefore, we compared the *mTR* expression levels in $mTERT^{+/+}$, $mTERT^{+/-}$ and $mTERT^{-/-}$ embryos to examine if the absence of *mTERT* gene expression *per se* has any effect on the *mTR* expression levels. Two independent littermates derived from intercrossing between $mTERT^{+/-}$ mice were collected, and each embryo was genotyped. In parallel, total RNAs were extracted from each embryo, and subjected to Northern blotting analysis for *mTR* expression and 7S RNA expression as a control. As shown in Fig. 4, the expression levels of *mTR* were essentially same in $mTERT^{+/+}$, $mTERT^{+/-}$ and $mTERT^{-/-}$ embryos. Therefore, in our system, the steady state levels of *mTR*

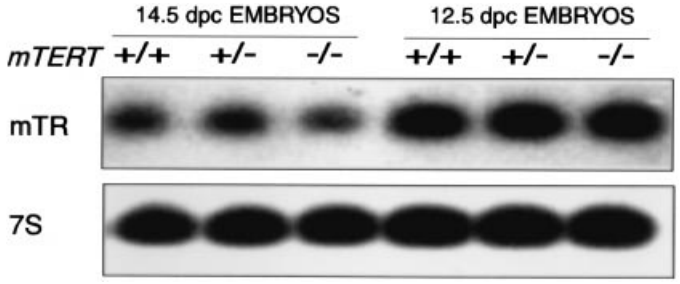

Figure 4 *mTR* expression in $mTERT^{+/+}$, $mTERT^{+/-}$ and $mTERT^{-/-}$ littermates. Embryos derived from $mTERT^{+/-}$ intercrosses were collected at 14.5 dpc and 12.5 dpc of development. Each embryo was genotyped, and total RNA was isolated and probed with the *mTR* cDNA (top). The same blot was rehybridized with the 7S RNA probe as an internal control (bottom).

expression was not significantly influenced by the lack of *mTERT* gene, suggesting that mTR metabolism is more or less independent of the production of mTERT protein.

Single-stranded telomeric G-tails in *mTERT*$^{-/-}$ mice

Telomeric DNA consists of tandem arrays of simple G-rich repeats, TTAGGG in vertebrates, including the human and the mouse. The 3′-ends of the G-rich strands are orientated towards the telomeric termini, whereas the C-rich strands are orientated towards the centromeric direction. It is known that single-stranded G-rich repeats have a 3′-overhang at the very ends of telomeric repeats (Klobutcher *et al.* 1981; Makarov *et al.* 1997; McElligott & Wellinger 1997; Wright *et al.* 1997). This G-tail is about 200 nt in the human (Makarov *et al.* 1997; Wright *et al.* 1997); and longer than 30 nt at the end of S phase in yeast (Wellinger *et al.* 1993; Wellinger *et al.* 1996). Deletion of the *TLC1* gene that encodes the telomerase template RNA in yeast did not lead to the removal of the G-tail (Dionne & Wellinger 1996; Wellinger *et al.* 1996). Moreover, G-tails were equally detected in both telomerase-positive and telomerase-negative human cells (McElligott & Wellinger 1997). Therefore, it has been suggested that the G-tails are not produced by 3′-extension of the G-strand by telomerase, but by processing of the C-strand after replication by a yet uncharacterized 5′-exonucleolytic activity. However, in these studies, different types of human cells having or lacking telomerase activities were compared, and it is not known whether G-tails are present similarly in one particular type of mammalian cells regardless of the presence or absence of telomerase. This question is particularly interesting because it has been proposed that telomerase may has a structural role in telomere maintenance, in addition to its well established catalytic role of elongating telomeres (Prescott & Blackburn 1997). *mTERT*-knockout mice gave us a good opportunity to examine this question. Accordingly, we next examined the structures of the telomeric repeats in the *mTERT*$^{-/-}$ cells.

In previous studies, the presence of the single-stranded G-tail was demonstrated by detecting telomeric signals in in-gel hybridization experiments under a nondenaturing condition (Dionne & Wellinger 1996; Mitchell *et al.* 1999). These signals were sensitive to single-stranded DNA specific 3′-exonuclease treatment of DNAs prior to restriction enzyme digestion. The single-strand-specific DNase removes the G-tail and the resultant completely double-stranded telomeric DNA does not hybridize with the probe in a nondenaturing condition. As the mouse genomic DNA typically has long telomeric repeats of about 50 kb, conventional Southern blotting analysis was not suitable for the examination of presence of G-tails in mouse cells. We therefore used pulse field gel electrophoresis (PFGE) to fractionate the restriction fragments containing telomeric repeats (TRF: terminal restriction fragment), and the TRFs were then hybridized with telomeric probes in nondenaturing and denaturing conditions. MEF cells and liver cells were obtained from the *mTERT*$^{+/+}$, *mTERT*$^{+/-}$ and *mTERT*$^{-/-}$ mice, and were suspended in PBS solution. They were embedded in agarose plugs, and were treated with proteinase K. The DNA within the agarose plugs was digested with *Hin*fI, and subjected to PFGE. During this procedure, the agarose plugs were always maintained at temperatures below 37 °C to avoid false positives caused by inadvertent DNA denaturation of short DNA duplexes. Mouse TRFs contain highly polymorphic subtelomeric repeats as well as long telomeric repeats (Kipling & Cooke 1990; Starling *et al.* 1990). Therefore, TRF signals detected by telomeric probes in PFGE typically show heterogeneous smears ranging from about 40 kb to 150 kb (data not shown). To minimize the difficulty of detecting hybridizing signals due to a smear distribution of TRFs in the gel, we have established a PFGE condition in which most TRFs migrate at the limiting mobility zone and are thus condensed. Ethidium bromide staining of gels indicated that the vast majority of the genomic DNA had migrated faster than TRFs (data not shown). The TRFs were then hybridized in the gel to the end-labelled $(CCCTAA)_4$ oligonucleotide probe at a nondenaturing condition, and were exposed to an X-ray film (Fig. 5A, NATIVE). After the DNA was denatured, the same gel was rehybridized using the same probe (Fig. 5A, DENATURED). As a control, similar experiments were performed using the end-labelled $(TTAGGG)_3$oligonucleotide probe (Fig. 5B).

The nondenaturing hybridization using the CCCTAA-probe gave significant signals in all of *mTERT* genotypes in both MEF and liver cells. These signals showed exactly the same mobility with TRF signals detected under the denaturing condition. Pretreatment of the agarose plugs by single-stranded DNA specific mung bean nuclease completely abolished the signals detected in the nondenaturing condition. In addition, when the nondenaturing hybridization was carried out using a probe of the opposite strand for telomere repeats $(TTAGGG)_3$,

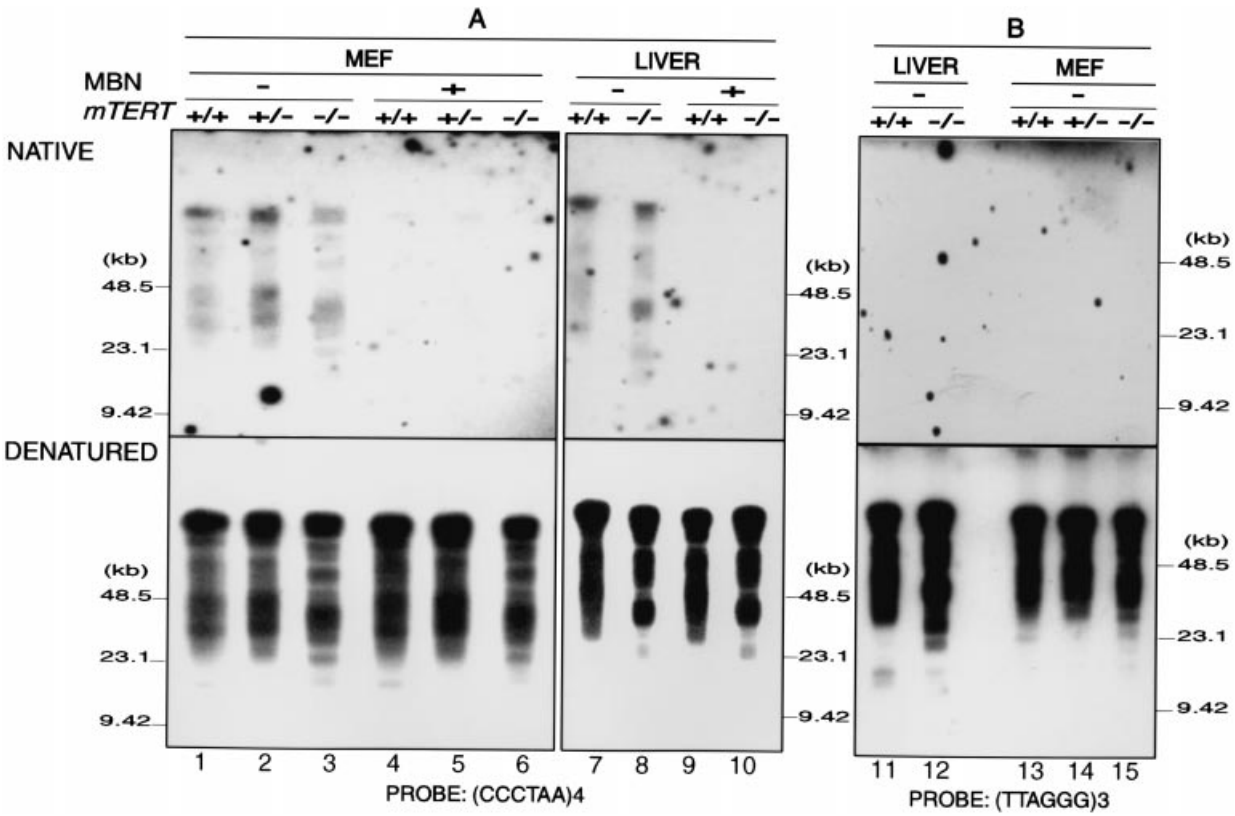

Figure 5 The G − tails are present in *mTERT*$^{+/+}$, *mTERT*$^{+/-}$ and *mTERT*$^{-/-}$ mice cells. Genomic DNAs derived from *mTERT*$^{+/+}$, *mTERT*$^{+/-}$, and *mTERT*$^{-/-}$ MEF and liver cells were digested with *Hin*fI, fractionated in PFGE and subjected to in-gel hybridization with the $(CCCTAA)_4$ oligonucleotide probe (A), or the $(TTAGGG)_3$ oligonucleotide probe (B), under the nondenaturing (native) or the denaturing (denaturing) condition. The gels were exposed to X-ray films that are shown here. MBN + or − indicates whether the DNAs were treated with mung bean nuclease prior to restriction digestions or not. The genotypes of the cells examined are shown by mTERT+/+, +/− and −/−.

no signal was detected in all of the mTERT genotypes (Fig. 5B, NATIVE). In a control experiment, a non-denaturing $(TTAGGG)_3$-hybridization in the same condition resulted in positive signals with 5 pg of denatured CCCTAA-repeated fragment having lengths of 1–2 kb (data not shown). Taken together, these results indicated that the G-tails are present in the MEF and mouse liver cells, and that these G-tails were not significantly changed in *mTERT*$^{+/+}$, *mTERT*$^{+/-}$ and *mTERT*$^{-/-}$ mice. Similar results were obtained in four independent experiments. Therefore, it was suggested that the G-tails might be formed by a telomerase-independent mechanism, as previously suggested for yeast and human cells.

Discussion

In this paper, we have reported the initial characterization of knockout mice deleted for the *mTERT* gene that encodes the catalytic subunit of the telomerase ribonucleotide-protein complex. All tissues derived from the *mTERT*$^{-/-}$ mice that were analysed showed no telomerase activity, formally indicating that the mTERT is the only catalytic component responsible for telomerase activity. In this study, we characterized the G1 and G2 *mTERT*$^{-/-}$ mice. They developed normally, showed no macroscopic or microscopic phenotypic changes, and were fertile. These results are similar to those observed for the *mTR*$^{-/-}$ mice, in which apparent abnormalities appeared only in G5 mice or those of later generations (Blasco *et al.* 1997; Lee *et al.* 1998). It is still possible that G1 or G2 *mTERT*$^{-/-}$ mice may show abnormal responses to certain types of stress, such as the application of cytotoxic drugs or radiation. Nevertheless, the lack of any serious abnormality in these animals under standard conditions suggests that the TERT protein is primarily responsible for the catalytic activity of

telomerase, and is not required for other vital functions, such as having a structural role at the telomeres. One thing we need to be cautious about is that it is possible that a truncated TERT protein is generated in our *mTERT*$^{-/-}$ mice, although it is extremely difficult to detect the TERT protein by Western blotting due to its very minute quantity. This catalytically inactive protein may be still active in terms of other functions, and may have masked phenotypes in our *mTERT*$^{-/-}$ mice. A More detailed examination will be necessary to exclude any additional role of the TERT protein.

Recently, the T-loop has been identified as a unique structure capping telomeres. The T-loop is formed by a triplex structure between duplex telomeric repeats and the terminal G-tail at the base of the loop (Griffith *et al.* 1999). Therefore, G-tails are essential for the higher-order telomere structure, and an understanding of how the G-tail is formed is an important issue. Telomerase elongates the G-strand in the 5′-to-3′ orientation, and it is possible that G-tails are indeed telomerase products. However, this possibility is unlikely, since G-tails were present in the yeast *tlc1* mutant which lacks the telomerase template RNA, at a similar level as that found in the wild-type yeast (Dionne & Wellinger 1996; Wellinger *et al.* 1996). Moreover, no change was observed in terms of G-tails in telomerase-negative and positive human cells (McElligott & Wellinger 1997). In this study, we found that G-tails are not influenced by *mTERT* deletion, further confirming the previous hypothesis.

In summary, this paper describes the establishment of *mTERT* knockout mice. This animal will be a good tool for determining the function of the TERT protein *in vivo*.

Experimental procedures

Gene targeting

A mouse 129Sv genomic library was screened using the mouse *TERT* cDNA as a probe, and several *mTERT* clones were isolated and mapped. A 14-kb *mTERT* genomic DNA fragment was subcloned and sequenced. Ten exons (designated as exons α through κ in Fig. 1A) encoding the amino acids 581–1005 of GENBANK accession number AF073311 were identified in this region. The targeting vector shown in Fig. 1A was constructed using pPolIIshort-neobPA-HSVTK (Ishibashi *et al.* 1993). The resulting targeting vector contained a neomycin resistant gene (neo) and two copies of Herpes simplex virus-thymidine kinase genes (HSV-TK) as the positive and the negative selection markers, respectively. 100 μg of the targeting vector was linearized and electroporated into 2×10^7 JH1 ES cells (a kind gift from J. Herz and R.E. Hammer, University of Texas South-Western Medical Center at Dallas, Dallas, Texas). ES cells that had undergone homologous recombination were screened by PCR using primers c and a (primer c located in the *neo* cassette, 5′-AGGATTGGGAAGACAATAGCAGGCAT-3′; primer a located in an intron upstream of the short homologous arm, 5′-GCGTGGAGTATCCTCCTGCATCTCTA-3′), and then verified by Southern blot analysis. The independent homologous-recombinant clones were injected into C57BL/6 blastocysts and chimera mice were generated. RT-PCR was performed with 1 μg of total RNAs extracted from adult testes of *mTERT*$^{+/+}$ and *mTERT*$^{-/-}$ mice using the primers 5′-2 and 3′-1 (primer 5′-2 located in exon α, 5′-CTTGAGAGAGTGCGGCTACGGGAGCT-3′; primer 3′-1 located in exon κ, 5′-AAGACCGACAGGAGCTTGT TCCGCAT-3′).

Telomerase activity measurement

Cytoplasmic S-100 extracts were prepared from cells and tissues and analysed by the stretch PCR assay as described (Tatematsu *et al.* 1996).

mTR Northern blot analysis

Total RNAs were prepared from 12.5 dpc and 14.5 dpc embryos of two independent *mTERT*$^{+/-}$ intercrossings using the Sepasol total RNA preparation reagent (Nakarai Co., Japan). 20 μg of total RNAs were subjected to Northern blot analysis. The probes used for Northern blot were as follows: *mTR* full length cDNA fragment (kindly provided by Yoichi Shinkai, Institute of Virus Research, Kyoto University), 5′ end-labelled DNA oligonucleotides complementary to mouse 7S RNA (5′-GTTGCCGAACTTAGTGCGG ACACC CGATCG-3′).

Detection of G-strand telomeric tails

High-molecular-weight genomic DNAs embedded in a agarose plug was prepared from MEF and liver cells as described (Birren *et al.* 1997) with the exception that the preparation of the agarose plugs and lysis of the cells within plugs were carried out at 37 °C. In some experiments, a plug was incubated in 400 U/mL of mung bean nuclease (Takara Co., Japan) at 25 °C for 1 h to remove single-strand DNAs. Plugs treated with or without mung bean nuclease were digested with *Hin*fI and separated in a 1% agarose gel in 0.5× TBE buffer maintained at 12 °C, using a CHEF-DR III pulse field system (Bio-Rad). Electrophoresis was carried out at 5 V/cm and at a constant pulse time of 3 s for 12 h. Native and denatured in-gel hybridization were carried out as described (McElligott & Wellinger 1997). The gel was first hybridized to the 5′ end-labelled oligonucleotide probe of $(CCCTAA)_4$, or $(TTAGGG)_3$ in a nondenaturing condition. After the signals were obtained, the DNA was denatured in the gel and hybridized to the same probe. Autoradiography to an X-ray film (Amersham) was carried out at −80 °C.

Histology

The mice were autopsied after being sacrificed according to the guidelines for animal experimentation. Brain, gastrointestinal tract, liver, pancreas, adrenals, hypophysis, submandibular glands, thyroid, parathyroid, thymus, spleen, bone marrow, reproductive organs, kidneys, lungs and heart were obtained, fixed in 4% formaldehyde and embedded in paraffin. Hematoxylin-Eosin stained 3 μm sections were examined microscopically.

Acknowledgements

We thank E.A. Kamei (Gunma University) for critical reading of and comments on the manuscript, and J. Osuga and R. Tozawa for valuable advice on the experiment. The excellent secretarial works of F. Nishizaki, K. Saito and K. Yokoyama, and excellent technical helps by K. Saito and M. Herai are acknowledged. This work was supported by a grant-in-aid from the Organization for Pharmaceutical Safety and Research, Japan.

References

Birren, B., Green, E.D., Klapholz, S., Myers, R.M. & Roskams, J. (1997) *Genome Analysis*: a Laboratory Manual, Cold Spring Harbor. New York. Cold Spring Harbor Laboratory Press.

Blasco, M.A., Funk, W., Villeponteau, B. & Greider, C.W. (1995) Functional characterization and developmental regulation of mouse telomerase RNA. *Science* **269**, 1267–1270.

Blasco, M.A., Lee, H.W., Hande, M.P., *et al.* (1997) Telomere shortening and tumor formation by mouse cells lacking telomerase RNA. *Cell* **91**, 25–34.

Chin, L., Artandi, S.E., Shen, Q., *et al.* (1999) p53 deficiency rescues the adverse effects of telomere loss and cooperates with telomere dysfunction to accelerate carcinogenesis. *Cell* **97**, 527–538.

Counter, C.M., Meyerson, M., Eaton, E.N. & Weinberg, R.A. (1997) The catalytic subunit of yeast telomerase. *Proc. Natl. Acad. Sci. USA* **94**, 9202–9207.

Dionne, I. & Wellinger, R.J. (1996) Cell cycle-regulated generation of single-stranded G-rich DNA in the absence of telomerase. *Proc. Nat. Acad. Sci. USA* **93**, 13902–13907.

Feng, J., Funk, W.D., Wang, S.S., *et al.* (1995) The RNA component of human telomerase. *Science* **269**, 1236–1241.

Greider, C.W. & Blackburn, E.H. (1985) Identification of a specific telomere terminal transferase activity in Tetrahymena extracts. *Cell* **43**, 405–413.

Greider, C.W. & Blackburn, E.H. (1989) A telomeric sequence in the RNA of Tetrahymena telomerase required for telomere repeat synthesis. *Nature* **337**, 331–337.

Griffith, J.D., Comeau, L., Rosenfield, S., *et al.* (1999) Mammalian telomeres end in a large duplex loop. *Cell* **97**, 503–514.

Harrington, L., McPhail, T., Mar, V., *et al.* (1997) A mammalian telomerase-associated protein. *Science* **275**, 973–977.

Ishibashi, S., Brown, M.S., Goldstein, J.L., Gerard, R.D., Hammer, R.E. & Herz, J. (1993) Hypercholesterolemia in low density lipoprotein receptor knockout mice and its reversal by adenovirus-mediated gene delivery. *J. Clin. Invest.* **92**, 883–893.

Kipling, D. & Cooke, H.J. (1990) Hypervariable ultra-long telomeres in mice. *Nature* **347**, 400–402.

Klobutcher, L.A., Swanton, M.T., Donini, P. & Prescott, D.M. (1981) All gene-sized DNA molecules in four species of hypotrichs have the same terminal sequence and an unusual 3′ terminus. *Proc. Natl. Acad. Sci. USA* **78**, 3015–3019.

Lee, H.W., Blasco, M.A., Gottlieb, G.J., *et al.* (1998) Essential role of mouse telomerase in highly proliferative organs. *Nature* **392**, 569–574.

Lingner, J., Hughes, T.R., Shevchenko, A., Mann, M., Lundblad, V. & Cech, T.R. (1997) Reverse transcriptase motifs in the catalytic subunit of telomerase. *Science* **276**, 561–567.

Makarov, V.L., Hirose, Y. & Langmore, J.P. (1997) Long G tails at both ends of human chromosomes suggest a C strand degradation mechanism for telomere shortening. *Cell* **88**, 657–666.

McElligott, R. & Wellinger, R.J. (1997) The terminal DNA structure of mammalian chromosomes. *EMBO J.* **16**, 3705–3714.

Meyerson, M., Counter, C.M., Eaton, E.N., *et al.* (1997) hEST2, the putative human telomerase catalytic subunit gene, is up-regulated in tumor cells and during immortalization. *Cell* **90**, 785–795.

Mitchell, J.R., Cheng, J. & Collins, K. (1999) A box H/ACA small nucleolar RNA-like domain at the human telomerase RNA 3′ end. *Mol. Cell. Biol.* **19**, 567–576.

Nakayama, J., Saito, M., Nakamura, H., Matsuura, A. & Ishikawa, F. (1997) TLP1: a gene encoding a protein component of mammalian telomerase is a novel member of WD repeats family. *Cell* **88**, 875–884.

Nakayama, J., Tahara, H., Tahara, E., *et al.* (1998) Telomerase activation by hTRT in human normal fibroblasts and hepatocellular carcinomas. *Nature Genet.* **18**, 65–68.

Nugent, C.I., Bosco, G., Ross, L.O., *et al.* (1998) Telomere maintenance is dependent on activities required for end repair of double-strand breaks. *Curr. Biol.* **8**, 657–660.

Prescott, J. & Blackburn, E.H. (1997) Functionally interacting telomerase RNAs in the yeast telomerase complex. *Genes Dev.* **11**, 2790–2800.

Shay, J.W. & Bacchetti, S. (1997) A survey of telomerase activity in human cancer. *Eur. J. Cancer* **33**, 787–791.

Starling, J.A., Maule, J., Hastie, N.D. & Allshire, R.C. (1990) Extensive telomere repeat arrays in mouse are hypervariable. *Nucl. Acids Res.* **18**, 6881–6888.

Tatematsu, K., Nakayama, J., Danbara, M., *et al.* (1996) A novel quantitative 'stretch PCR assay', that detects a dramatic increase in telomerase activity during the progression of myeloid leukemias. *Oncogene* **13**, 2265–2274.

Weinrich, S.L., Pruzan, R., Ma, L., *et al.* (1997) Reconstitution of human telomerase with the template RNA component hTR and the catalytic protein subunit hTRT. *Nature Genet.* **17**, 498–502.

Wellinger, R.J., Ethier, K., Labrecque, P. & Zakian, V.A. (1996) Evidence for a new step in telomere maintenance. *Cell* **85**, 423–433.

Wellinger, R.J., Wolf, A.J. & Zakian, V.A. (1993) Saccharomyces telomeres acquire single-strand TG1–3 tails late in S phase. *Cell* **72**, 51–60.

Wright, W.E., Tesmer, V.M., Huffman, K.E., Levene, S.D. &

Shay, J.W. (1997) Normal human chromosomes have long G-rich telomeric overhangs at one end. *Genes Dev.* **11**, 2801–2809.

Yi, X., Tesmer, V.M., Savre-Train, I., Shay, J.W. & Wright, W.E. (1999) Both transcriptional and posttranscriptional mechanisms regulate human telomerase template RNA levels. *Mol. Cell. Biol.* **19**, 3989–3997.

Yu, G.L., Bradley, J.D., Attardi, L.D. & Blackburn, E.H. (1990) In vivo alteration of telomere sequences and senescence caused by mutated Tetrahymena telomerase RNAs. *Nature* **344**, 126–132.

Received: 5 August 1999
Accepted: 17 August 1999

